Chapter 2

Experimental Section

2. Experimental Section

This chapter covers the details of the all chemicals used during the experiments and the entire experimental techniques along with all characterization technique that have used in the present study are briefly explained.

2.1. Materials and Reagents used

All the chemicals used during the experiments are listed herein Table 2.1. The whole chemicals are used as received without further purification. In all experiments distilled water was used.

Table 2.1 List of Chemicals

Chemicals	Purchased from
Copper(II) chloride dihydrate ($CuCl_2 \cdot 2H_2O$, 99%), Cobalt(II) chloride hexahydrate ($CoCl_2 \cdot 6H_2O$, 99%), Iron (II) chloride ($FeCl_2$. $4H_2O$, 99%), Iron (III) chloride hexahydrate ($FeCl_3$. $6H_2O$, 99%), Nickel (II) Chloride ($NiCl_2$, 99%), Palladium(II) chloride ($PdCl_2$, 99.0%), Ethanol, Formic acid (HCOOH; 100%), Hydrazine hydrate (85%), Potassium hydroxide (KOH), Sodium hydroxide (NaOH), Sodium borohydride ($NaBH_4$), 2-Propanol {$(CH_3)_2CHOH$}	Merck, India
4-nitrophenol (4-NP) , 4-nitroaniline (4-NA), 3-nitroaniline (3-NA), 2-nitroaniline (2-NA), 4-nitrotoluene, 4-chloronitrobenzene, 4-bromo nitrobenzene, 3-bromo nitrobenzene, 4-iodo nitrobenzene, 3-iodo nitrobenzene, 4-floro nitrobenzene	SRL, India
Nafion, 20 wt% Pt/C, 20 wt % Pd/C	Alfa Aesar
Vulcan XC-72 R, Carbon powder	Cabot Corp.

2.2. Synthesis of the Catalysts

2.2.1. Synthesis of Different Composition of Bimetallic $Pd_{4-x}Fe_x/C$ (x = 1, 2 and 3) and $Pd_3Fe_{0.5}Cu_{0.5}/C$ Nanoparticles (NPs)

Synthesis of $Pd_3Fe_{0.5}Cu_{0.5}/C$ NPs: The 20 wt% of $Pd_3Fe_{0.5}Cu_{0.5}/C$ NPs was synthesized by the typical solvothermal method [1-3]. To prepare the NPs, to a mixture solution of 25 mL distilled water and 25 mL C_2H_5OH was mixed, 0.197 mmol $PdCl_2$ (0.0350 g), 0.065 mmol $FeCl_2{\cdot}4H_2O$ (0.0132 g), 0.065 mmol $CuCl_2{\cdot}2H_2O$ (0.0112 g), and 0.1 g Vulcan XC-72 R were added sequentially at room temperature with constant stirring. The mixture solution was ultra-sonicated for 5 min and 30 mL 0.05 M (0.2 g) NaOH solution was added dropwise at room temperature under constant stirring. After ca. 20 min, 2 mL 85% hydrazine hydrate was added dropwise to the mixture and stirred vigorously for another 25 min. The solution was then transferred into a Teflon cup (250 mL capacity) in a stainless steel autoclave. The autoclave was sealed and kept in an oven at 120 °C for 6 h and allowed to cool naturally (~2.5 h); the final product was washed several times with distilled water and then 50% C_2H_5OH to remove the unreacted NaOH and Cl^-, and finally collected by centrifugation. The product was dried in a vacuum oven at 55 °C.

Synthesis of $Pd_{4-x}Fe_x/C$ NPs: The synthesis procedures for $Pd_{4-x}Fe_x/C$ NPs (x = 1, 2 and 3) were similar to that of $Pd_3Fe_{0.5}Cu_{0.5}/C$ NPs keeping other conditions unaltered and only varying the initial mole ratio of Pd and Fe salt precursors to 1:3, 1:1 and 3:1.

Synthesis of Pd/C NPs: The Pd/C NPs were also synthesized using the method similar to that for $Pd_3Fe_{0.5}Cu_{0.5}/C$. In this case, only $PdCl_2$ was employed as the metal precursor.

2.2.2. Synthesis of $Pd_3Cu_{0.5}Ni_{0.5}/C$ and Pd_2CuCo/C NPs

$Pd_3Cu_{0.5}Ni_{0.5}/C$ and Pd_2CuCo/C NPs were synthesized by the same procedure as mentioned in the section 2.2.1. by changing the appropriate precursor solutions and mole ratios.

2.2.3. Synthesis of Cu-$CuFe_2O_4$/C NPs

The 20 wt% of Cu-$CuFe_2O_4$/C was synthesized by the typical solvothermal synthesis method. To prepare the NPs to 25 mL distilled water and 25 mL C_2H_5OH was mixed, then add 0.21 mmol $CuCl_2.2H_2O$ (0.0359 g), 0.21 mmol $FeCl_2.4H_2O$ (0.0419 g) and 0.1 g Vulcan XC-72 R at room temperature, after that sonicated the solution for 5 min, then 30 mL 0.006 M (0.2 g) NaOH solution was added drop wise at room temperature under constant stirring. After about 20 min, 2 mL of 85% hydrazine hydrate was added drop wise to the mixture and stirred vigorously. After about 25 min the solution was transferred into a Teflon cup (250 mL capacity) in a stainless steel autoclave. The autoclave was sealed and kept in an oven at 120 ^oC for 6 h. The autoclave was allowed to cool naturally (~2.5 h); the final product was washed several times with distilled water and then 50% C_2H_5OH solution to remove the unwanted NaOH and Cl^- and finally collected by centrifugation. The product was dried in a vacuum oven at 55 ^oC.

Synthesis of $CuFe_2O_4$/C: The 20 wt% $CuFe_2O_4$/C NPs are prepared using same procedure as Cu-$CuFe_2O_4$/ C NPs without using hydrazine hydrate.

Synthesis of Cu-$CuFe_2O_4$: The bare composition Cu-$CuFe_2O_4$ NPs was synthesized using same procedure as Cu-$CuFe_2O_4$/C, without adding the Vulcan carbon.

Synthesis of Cu-$CuFe_2O_4$ + C: The Cu-$CuFe_2O_4$ + C were prepared by using bare Cu-$CuFe_2O_4$ and Vulcan carbon by mixing through sonication.

2.2.4. Synthesis of CuCo/$CuOCo_3O_4$/C NPs

The CuCo/$CuOCo_3O_4$/C NPs were also synthesized using the method similar to that for Cu-$CuFe_2O_4$/C. In this case, calculated amount of $CuCl_2{\cdot}2H_2O$ and $CoCl_2{\cdot}6H_2O$ were employed as the metal precursors.

Synthesis of Monometallic Cu/C and Co/C: The monometallic Cu/C and Co/C NPs were synthesized by following procedure as mentioned in the section 2.2.4 with single metal precursor.

Synthesis of $CuOCo_3O_4$/C: The $CuOCo_3O_4$/C NPs are prepared using same procedure as Cu-$CuFe_2O_4$/ C NPs without using hydrazine hydrate.

Synthesis of $CuCo/CuOCo_3O_4$: The $CuCo/CuOCo_3O_4$ NPs was synthesized using same procedure as Cu-$CuFe_2O_4$/C, without adding the Vulcan carbon.

Synthesis of $CuCo/CuOCo_3O_4$ + C: The $CuCo/CuOCo_3O_4$+ C were synthesized by using bare Cu-$CuFe_2O_4$ and Vulcan carbon by mixing through sonication.

2.2.5. Synthesis of Cu NPs

Cu NPs were synthesized by the typical hydrothermal synthesis method. To prepare the Cu NPs 50 mL aqueous solution of 0.850 g (200 mM) $CuCl_2.2H_2O$ was added to 50 mL NaOH solution dropwise (0.8 g, 0.4 M) at room temperature under constant stirring. After stirring about 20 min, 3.5 mL of 85% hydrazine hydrate was added drop wise to the mixture and stirred vigorously. After about 25 min the solution was transferred into a Teflon cup (250 mL capacity) in a stainless steel autoclave. The autoclave was sealed and kept in an oven at 120 °C for 6 h. The autoclave was allowed to cool naturally (~2.5 h); a deep red wine fluffy solid product was deposited on the bottom of the Teflon cup which indicates the formation of Cu NPs. The final product was washed several times with distilled water and then 50% C_2H_5OH solution to remove the unwanted NaOH and Cl^-, and finally collected by centrifugation. The product was dried in a vacuum oven at 55 °C [4,5].

Synthesis of Iron Oxide NPs

To prepare the FeO_x NPs 50 mL aqueous solution of 1.350 g (200 mM) $FeCl_3.6H_2O$ was added to 50 mL NaOH solution (0.8 g, 0.4 M) at room temperature under constant stirring. After stirring about 20 min, 3.5 mL of 85% hydrazine hydrate was added drop wise to the mixture and stirred vigorously. The remaining procedure is identical to the synthesis of Cu NPs.

Synthesis of Cu/Fe_2O_3 NPs

To synthesize Cu/Fe_2O_3 NPs, 50mL aqueous solution of required amount of $CuCl_2.2H_2O$ (0.426 g) and $FeCl_3.6H_2O$ (0.405 g) were added to 50 mL NaOH solution (0.8 g, 0.4 M) at room temperature under constant stirring. After stirring about 15 min, 3.5 mL of 85% hydrazine hydrate was added drop wise to the mixture and stirred vigorously. The remaining procedure is identical to the synthesis of Cu NPs.

2.2.6. Synthesis of CuNi NPs

In a typical procedure, to prepare CuNi, 50 mL aqueous solution of 0.552 g (120 mM) $CuCl_2 \cdot 2H_2O$ and 0.475 g (80 mM) $NiCl_2 \cdot 6H_2O$ is added to 50 mL NaOH solution (0.8 g, 0.4 M) at room temperature under constant stirring. After stirring about 15 min, 3.5 mL of 85% hydrazine hydrate was added dropwise to the mixture and stirred vigorously. After about 20 min the solution was transferred into a Teflon cup (250 mL capacity) in a stainless steel autoclave. The autoclave was sealed and kept in an oven and maintained at 120 °C for 6 h. The autoclave was allowed to cool naturally (~2.5 h); a black fluffy solid product was deposited on the bottom of the Teflon cup which indicates the formation of CuNi bimetallic NPs. The final product was washed several times with distilled water and then 50% C_2H_5OH solution to remove the unreacted NaOH and Cl^-, and finally collected by centrifugation. The product was dried in a vacuum oven at 55 °C for 12 h.

Synthesis of Ni NPs:

Identical procedure was employed to prepare Ni NPs as mentioned in 2.2.6 employing appropriate Ni salt precursor.

2.3. Characterization Techniques

2.3.1. Thermogravimetric Analysis (TGA)

The loss or gain in weight of a sample as a function of temperature is measured by thermogravimetric analysis. It is extremely helpful technique to study solid-gas systems. When a matter is subjected to a programmed as a function of temperature, it normally undergoes chemical, physical or mechanical changes. As the main parameter of the characterization technique is temperature, therefore the common name is

thermogravimetry. The TGA instruments have an ultra-sensitive weighing tool. The changes in the mass of the sample clearly imply loss or gain of matter by the sample. All the TGA curves represented in this thesis work were obtained on a Thermal Analyzer (Model TGA-50, Shimadzu) instrument. The samples were heated from room temperature to 700^{o}C under air atmosphere. The heating rate in each case was kept at 10 ^{o}C min^{-1} [6,7].

2.3.2. X-ray Powder Diffraction (XRD)

X-ray diffraction (XRD) was used to study the structure parameter of non amorphous material. Normally, it provides the information about the phase of the sample, crystallinity and crystallite size of the materials. The XRD technique is based on the Bragg's law $n\lambda = 2d\sin\theta$, where, d is the lattice spacing, λ is the wavelength of X-ray beam , θ is the angle of the X-ray beam with respect to the lattice plane, and n is the order of lattice planes. When the incoming a collimated beam of X-ray beams diffracted with a suitable angle with the lattice plane (Figure 2.1), the rays diffract coherently from the lattice planes, the X-rays mutually reinforce each other and produce a peak. The Position, intensity and width of the peak gives the required information about the samples. The all (XRD) patterns were recorded on a Bruker AXS Model D8 focus instrument using nickel-filtered CuK_{α} (0.15418 nm) radiation source at the 2θ between 10° and 80°, the scan rate was 0.05° s^{-1} [8-10].

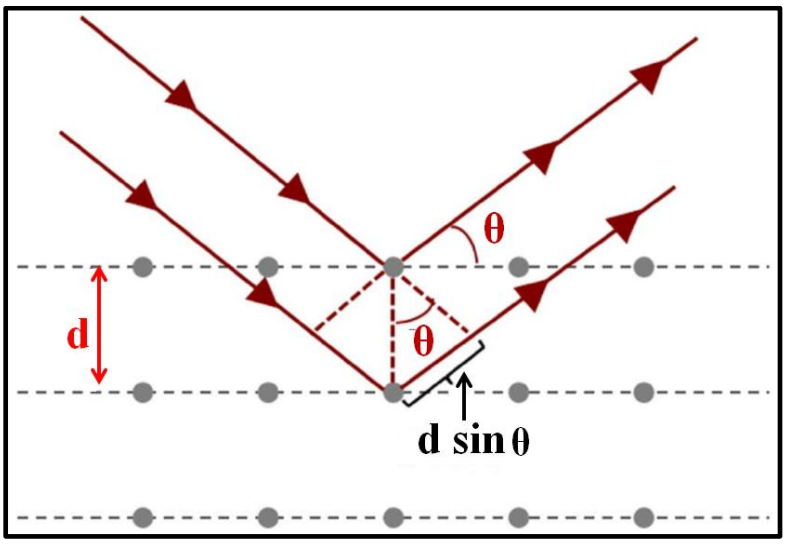

Figure 2.1 Schematic illustration of Bragg's law.

The crystallite size were determined by using Scherrer equation as mentioned below-

$$D = K \lambda / \beta \cos \theta \qquad (1)$$

Where, λ is the wavelength of X-ray source (CuKα = 0.15418 nm), β is the full width at half maximum (FWHM), θ is the diffraction angle, K is shape factor, D is mean size of the ordered (crystalline) domain.

2.3.3. Ultraviolet-Visible (UV-Visible) Spectroscopy

Ultraviolet-visible spectroscopy (UV-Vis) refers to absorption spectroscopy or reflectance spectroscopy in the ultraviolet-visible spectral region in the electromagnetic spectrum [11,12]. In this region, molecules experience electronic transitions. The working principle of a UV-Vis spectroscopy is based on the Beer-Lambert law (A = εCl) where, A = absorbance, ε = molar absorption coefficient, C = concentration of the solution and l = length of the solution the light pass through. UV-vis technique generally measures the intensity of incident light (I_o) *vs.* the intensity of light (I) passing through a sample. The ratio (I/I_o) is known as the transmittance and is normally expressed as percentage of transmittance (%T). In this present work, UV-Vis spectra were taken on a UV-visible spectrophotometer, Shimadzu Corporation (UV-2550).

2.3.4. Scanning Electron Microscopy (SEM)

The scanning electron microscope (SEM) is a vital technique to investigate the morphological quality of materials. The SEM is a type of electron microscope that images the sample surface by scanning it with a high-energy probe of electrons (5-50 eV) in a raster scan pattern. Since of its flexibility and the broad range of information SEM can give, the SEM is frequently the preferred starting instrument for analytic microscopy [13]. The Interaction of the electron beam with the specimen surface, causing a variety of signals; secondary electrons, backscattered electrons, X-rays, photons, which produces different types of signals providing detailed information about the surface structure and morphology of the specimen. To study the surface morphology, SEM analyses were carried out with "JEOL, JSM Model 6390 LV" scanning electron microscope, operating at an accelerating voltage of 15 kV. EDX as

well as EDS elemental mapping analyses can help to obtain more chemical and electronic information at the sub nanometer scale. This analysis was also performed in the same instrument attached to the scanning electron microscope.

2.3.5. Transmission Electron Microscopy (TEM)and High Resolution Transmission Electron Microscopy (HR-TEM)

TEM and HR-TEM investigations were performed on a FEI-Technai (G2 20 S-TWIN) instrument equipped with a slow-scan CCD camera and at an accelerating voltage of 200 kV. The samples were prepared by dispersing the samples in suitable solvents like ethanol, DCM, isopropanol, acetone etc. After that a drop of dispersed samples were placed on carbon coated copper grids and allowing them to dry [14,15].

2.3.6. Surface Area, Pore Size, Pore Volume (BET and BJH Method)

Specific surface area, average pore diameter, pore volume of different samples were measured by using Quantachrome instruments (Model: NOVA 1000e). The Brunauer-Emmett-Teller (BET) calculation was applying to calculate surface area of the catalyst by adsorption of N_2 gas at 77 K. N_2 vapour adsorption data was obtained for the vapour pressure range (p/p_o) of 0.03 to 0.3. The samples were degassed at 100 ^oC for 3 h under helium before subjecting the samples for N_2 adsorption, Pore size distributions were derived from desorption isotherms using the Barrett-Joyner-Halenda (BJH) method [16].

2.3.7. Gas Chromatography-Mass Spectrometry (GC-MS)

Gas chromatography-mass spectrometry is basically used to identify different substances present in a sample. In GC the particular sample is carried by an inert gas through the capillary column. Based on the “retention time” the samples can be identified compared with the reference value [17]. The sample is then fragmented by the effect of electron in Mass Spectrometry giving rise to the mass of that fragmented ions. Depending upon the fragmentation pattern the compound of the particular interest can be identified. In our present investigation the GC-MS analysis were done by a Perkin Elmer, USA (Model: Clarus 600) instrument. After the completion of the reaction, the organic substances were separated and used for the analysis.

2.3.8. X-Ray Photoelectron Spectroscopy (XPS)

X-ray Photoelectron Spectroscopy is a surface sensitive quantitative surface sensitive technique based on photoelectric effect. It gives the elemental composition and the chemical states of the elements present within the material [18,19]. For our investigation, the XPS studies were performed using a Thermo K-Alpha XPS equipped with an Al Kα radiation (1486.6 eV) X-ray source at a pressure < 10^{-7} Torr and an electron take-off angle (angle between electron emission direction and surface plane) of 90°. A survey scan was performed using pass energy of 200 eV to determine possible contaminants. The binding energies of the samples were charge-corrected with respect to the adventitious carbon (C 1s) peak at 284.6 eV.

2.3.9. Inductively Coupled Plasma-Optical Emission Spectrometry (ICP-OES)

Inductively coupled plasma-optical emission spectrometer is an analytical tool used for the detection of metals present in a compound. It provides quantitative bulk elemental composition of different solid, liquid and powder samples as well [20]. In a typical procedure, for our investigation the solid sample was digested or dissolved in diluted nitric acid solution. The resulting sample solution was then analyzed with a Perkin Elmer, USA (Model: Optima 2100 DV) instrument. ICP-OES is especially a powerful and quantitative technique to analyze the chemical composition a sample.

2.3.10. Electrochemical Characterization

The electrochemical characterizations were performed by using cyclic voltammetry (CV), rotating disc electrode (RDE) and chronoamperometry (CA) measurement with the help of PGSTAT 204 electrochemical workstation, Metrohm, Autolab, The Netherlands.

2.3.10.1. Cyclic Voltammetry (CV)

Cyclic voltammetry is one of most extensively used electrochemical study which provides characteristic current-potential plots for the used electrode material. It is mostly a three electrode system where potential of the working electrode is measured against a reference electrode whose potential is usually known or fixed. On the basis of Nernst equation, the potentiometric measurements can be calculated [21].

The electrocatalytic oxygen reduction activities of the freshly prepared nanoparticles were measured following a typical procedure. In brief, glassy carbon (GC) electrode (3 mm diameter, GCE was polished with 0.005-μm Al_2O_3 powder. A typical suspension of the carbon-supported catalysts was prepared by adding 5 mg of fresh catalyst to 0.5 mL 2-propanol, deionized water and 0.5% Nafion solution, respectively. The resultant mixture was sonicated for 30 min until it became a uniform dark ink. Then, 3-5 μL of the suspension was quantitatively deposited onto the surface of the polished GC electrode (3 μL for Pd-based and 5 μL for Cu-based catalyst). The electrode coated with a thin film of the ink was dried at 35 °C under N_2 atmosphere for 6 h under vacuum. The modified GC electrode was inserted into an electrochemical cell and used as the working electrode. The cell includes two additional electrodes: a KCl saturated Ag/AgCl (Metrohm) as the reference electrode and a platinum wire (Metrohm) as the counter electrode. CV was performed using a computer-controlled electrochemical analyzer (Metrohm Autolab PGSTAT204 workstation, The Netherlands) at room temperature. The CV was measured in high purity N_2- and O_2-saturated (0.1 M KOH and 0.5 M H_2SO_4) solution with scan rate 50 mV s^{-1}. However, for the cleaning of the working electrode cycles of CV was recorded at a scan rate of 100 mVs^{-1} in N_2-atmosphere.

2.3.10.2. Rotating Disc Electrode (RDE) Measurements

To evaluate the kinetics of the ORR, rotating disc electrode (RDE) measurements was carried out [22]. RDE measurements were performed in O_2-saturated 0.1 M KOH. Oxygen was purged for at least 30 min before measurement and continuously bubbled through the electrolyte, in order to ensure the saturation of the electrolyte with O_2 and then blanketing the solution with an O_2 atmosphere during the entire experiment and all experiments were performed at room temperature.

To assess the kinetics of the electrochemical reactions RDE measurement was carried out at different rotating rates as 400, 900, 1600, 2500 and 3600 rpm. Koutecky-Levich (K−L) equation is used to calculate the number of electrons transferred during the ORR process.

The K−L equation is expressed as

$$\frac{1}{j} = \frac{1}{j_k} + \frac{1}{B\,\omega^{0.5}} \quad (2)$$

$$B = 0.62\ nF(Do_2)^{2/3}\nu^{-1/6}\ Co_2 \quad (3)$$

Where j is the current density, j_k is the kinetic current density, ω is the rotating rate of the electrode and B is the slope which could be obtained from the K−L plots. F is the Faraday constant (96500 C mol^{-1}), Do_2 is the diffusion co-efficient of O_2 in 0.1 M KOH (2.0 x 10^{-5} cm^2 s^{-1}), ν is the kinetic viscosity (0.01 cm^2 s^{-1}), Co_2 is the bulk concentration of O_2 (1.2 x 10^{-6} mol cm^{-3}) and the value of "n" represents the number of transferred electron in the ORR. All the data were collected at a scan rate of 10 mv s^{-1}. The electrochemical active surface area (ECSA) of the catalysts was evaluated by CVs in a N_2-saturated 0.1 M KOH solution. For Pd-based catalysts, to evaluate the ECSA of the samples the columbic charge for the reduction of Pd−O monolayer, formed on Pd catalysts at the forward scan, was applied. The ECSA were calculated using the following equation: ECSA = Q/SL, where L is the Pd loading, Q is the collected charge that calculated from the Pd−O stripping, and S is a constant of 210 μC cm^{-2} that assumes a monolayer of Pd−O on the surface. The stability of the ORR electrode was tested using chronoamperometry. The chronoamperometric response for the ORR was obtained at −0.3 V (*vs.* Ag/AgCl) of in O_2-saturated 0.1 M KOH solution at 1600 rpm. For comparison, a commercial 20 wt % Pd/C and Pt/C (Alfa Aesar) were measured under the identical experimental conditions.

2.4. Catalytic Activity

2.4.1. Kinetics of Catalytic Reduction of Nitroaromatics

The catalytic reduction of 4-Nitrophenol (4-NP) was carried out in a beaker with constant stirring (600 rpm) in the presence of monometallic or bimetallic catalysts and aq. $NaBH_4$ as reducing agent. In a typical procedure, to 20 mL (0.1 mmol L^{-1}) aqueous 4-NP purged with N_2 (to remove the dissolved oxygen) 5 mL (20 mmol L^{-1}) freshly prepared $NaBH_4$ was added. The 4-NP solution exhibits a strong absorption peak at ~315 nm in neutral or acidic conditions. Upon the addition of $NaBH_4$ solution, the absorption peak of 4-NP shifts from 315 to 400 nm immediately, which corresponded to a colour change of light yellow to yellow-green due to the formation

of 4-nitrophenolate ion. After the addition of NPs, the colour of the 4-nitrophenolate ions diminishes after different time intervals for various NPs. Meanwhile, the characteristic absorption peak of 4-nitrophenolate ion at 400 nm gradually decreases, while a new peak at ~300 nm develops which is ascribed to 4-aminophenol (4-AP).

In this experiment, the concentration of the borohydride ion, largely exceeds that of 4-NP. The metal NPs started the catalytic reduction by relaying electrons from the donor BH_4^- to the acceptor 4-NP right after the adsorption of both onto the particle surfaces. As the initial concentration of $NaBH_4$ was very high, it remained essentially constant throughout the reaction. For the evaluation of the catalytic rate, the pseudo-first-order kinetics with respect to 4-NP is a reasonable assumption. In this light, since the ratio of absorbance A_t of 4-NP at time 't' to its value A_0 measured at t = 0 must be equal to the concentration ratio C_t/C_0 of 4-NP, the kinetic equation for the reduction can be written as

$$dC_t/dt = -K_{app}C_t \quad \text{or} \quad \ln(C_t/C_0) \text{ or } \ln(A_t/A_0) = -K_{app}t \qquad \ldots\ldots(4)$$

Where, C_t is the concentration of 4-NP at time 't' and K_{app} is the apparent rate constant, which can be obtained from the decrease of the peak intensity at 400 nm with time. The apparent rate constant of this catalytic reaction in the presence of different NPs are measured from the plot of ln (A_t/A_0) *vs.* time.

2.4.2. Chemoselective Reduction of Nitroaromatics

In a typical procedure, 1.0 mmol of nitroaromatic substrate was taken in a two neck round bottom flask dispersed in 15 mL of distilled water. To this aqueous suspension, 3 mmol of $NaBH_4$ and the synthesised NPs (5 wt% of the nitro-substrate) were added. The contents were then kept under constant stirring at the rate of 500-700 rpm at room temperature. Progress of the reaction was monitored by thin layer chromatography (TLC). After the completion of the reaction, the NP was separated from the reaction mixture by an external magnet. The catalyst was first washed with distilled water (3 x 15 mL) to remove the excess borohydride and then with acetone (3 x 15 mL) to eliminate any traces of organic substance. The filtrate was dried using a rotary evaporator and the remaining mass containing the reaction mixture was

extracted with HPLC grade ethyl acetate (3 x 20 mL) and dried over anhydrous Na_2SO_4, the conversion/selectivity and product identification were done by GC-MS analysis.

2.4.3. Catalytic Transfer Hydrogenation Reaction

1 mmol of the reactant was dissolved in 10 mL 2-propanol followed by addition of 15 wt % of catalyst and 3 mmol KOH to a two-neck 100 mL round bottom flask. The reaction mixture was refluxed at 83 °C for the required time period. The progress of the reaction was monitored by TLC. After the completion of the reaction, the catalyst was separated from the reaction mixture by an external magnet. The catalyst was first washed with distilled water (3 x 15 mL) to remove the excess base and then then with acetone (3 x 15 mL) to eliminate any traces of organic substance. The filtrate was dried using a rotary evaporator and the remaining mass containing the reaction mixture was extracted with HPLC grade ethyl acetate (3 x 20 mL) and dried over anhydrous Na_2SO_4, the conversion/selectivity and product identification were done by GC-MS analysis.

References

[1] Byrappa, K., and Yoshimura, M. *Handbook of Hydrothermal Technology*. William Andrew, 2012.

[2] Li, Jianlin, Wu, Q., and Wu, J., Synthesis of nanoparticles via solvothermal and hydrothermal methods. *Handbook of Nanoparticles*, 295−328, 2016.

[3] Morey, G. W. Hydrothermal synthesis. *Journal of the American Ceramic Society*, 36(9):279−285, 1953.

[4] Borah, B. J., and Bharali, P. Surfactant-free synthesis of CuNi nanocrystals and their application for catalytic reduction of 4-nitrophenol. *Journal of Molecular Catalysis A: Chemical*, 390:29−36, 2014.

[5] Borah, B. J., Mahanta, A., Mondal, M., Gogoi, H., Yamada, Y., and Bharali, P. Cobalt-copper nanoparticles catalyzed selective oxidation reactions: efficient catalysis at room temperature. Chemistry Select, 3(34):9826−9832, 2018.

[6] Horowitz, H. H., and Metzger, G. A New analysis of thermogravimetric

traces. *Analytical Chemistry* 35(10):1464−1468, 1963.

[7] Bom, D., Andrews, R., Jacques, D., Anthonny, J., Chen, B., Meier, M. S., and Selegue, J. P. Thermogravimetric analysis of the oxidation of multiwalled carbon nanotubes: evidence for the role of defect sites in carbon nanotube chemistry. *Nano Letters* 2(6):615−619, 2002.

[8] Wikipedia Contributors. *Bragg law*. Retrieved on 19 July. 2019 from https://en.wikipedia.org/wiki/Bragg%27s_law July 2019.

[9] Ludwig, W., Reischig, P., King, A., Herbig, M., Lauridsen, E. M., Johnson, G., Marrow, T. J., and Buffiere, J. Y. Three-dimensional grain mapping by x-ray diffraction contrast tomography and the use of Friedel pairs in diffraction data analysis. *Review of Scientific Instruments*, 80(3):033905, 2009.

[10] He, B. B. *Two-dimensional X-ray diffraction*. John Wiley & Sons, 2011.

[11] Giusti, M. M., and Wrolstad, R. E. Characterization and measurement of anthocyanins by UV-visible spectroscopy. Current protocols in food analytical chemistry, 1, 2001.

[12] Forster, H. UV/Vis spectroscopy. Characterization I: 2734−2734, 2004.

[13] Joy, D. C. *Scanning Electron Microscopy*. Wiley-VCH Verlag GmbH & Co. KGaA, 2006

[14] Carter, C. B., and Williams, D. B. *Transmission Electron Microscopy*. Springer-Verlag US, 173−193, 2009.

[15] Kohl, H., and Reimer, L. *Transmission Electron Microscopy*. Springer, 2008.

[16] Brunauer, S., Emmett, P. H., and Teller, E. Adsorption of gases in multimolecular layers. *Journal of the American Chemical Society*, 60(2):309−319, 1938.

[17] Daferera, D. J., Ziogas, B. N., and Polissiou, M. G. GC-MS analysis of essential oils from some Greek aromatic plants and their fungitoxicity on Penicillium digitatum. *Journal of Agricultural and Food Chemistry*, 48(6):2576−2581, 2000.

[18] Wagner, C. D. *Handbook of X-ray Photoelectron Spectroscopy*. Ed. G. E. Muilenberg. Perkin-Elmer, 1979.

[19] Brriggs, D., and Seah, M. P. Practical surface analysis: Auger and X-ray Photoelectron Spectroscopy 1, 1990.

[20] Barnard, T. W., Crockett, M. I., Ivaldi, J. C., Lundberg, P. L., Yates, D. A., Levine, P. A., and Sauer, D. J. Solid-state detector for ICP-OES. *Analytical Chemistry,* 65(9):1231−1239, 1993.

[21] Nicholson, R. S., Theory and application of cyclic voltammetry for measurement of electrode reaction kinetics. *Analytical Chemistry,* 37(11):1351−1355, 1965.

[22] Opekar, F., and Beran, P. Rotating disk electrodes. *Journal of Electroanalytical Chemistry and Interfacial Electrochemistry*, 69(1):1−105, 1976.